Check for updates

How to cite: *Angew. Chem. Int. Ed.* **2023**, *62*, e202314531
doi.org/10.1002/anie.202314531

Peptides

Side-Chain Chemistry Governs Hierarchical Order of Charge-Complementary β-sheet Peptide Coassemblies

*Renjie Liu[+], Xin Dong[+], Dillon T. Seroski[+], Bethsymarie Soto Morales, Kong M. Wong, Alicia S. Robang, Lucas Melgar, Thomas E. Angelini, Anant K. Paravastu, Carol K. Hall, and Gregory A. Hudalla**

Abstract: Self-assembly of proteinaceous biomolecules into functional materials with ordered structures that span length scales is common in nature yet remains a challenge with designer peptides under ambient conditions. This report demonstrates how charged side-chain chemistry affects the hierarchical co-assembly of a family of charge-complementary β-sheet-forming peptide pairs known as CATCH(X+/Y−) at physiologic pH and ionic strength in water. In a concentration-dependent manner, the CATCH(6K+) (Ac-KQKFKFKFKQK-Am) and CATCH(6D−) (Ac-DQDFDFDFDQD-Am) pair formed either β-sheet-rich microspheres or β-sheet-rich gels with a micron-scale plate-like morphology, which were not observed with other CATCH(X+/Y−) pairs. This hierarchical order was disrupted by replacing D with E, which increased fibril twisting. Replacing K with R, or mutating the N- and C-terminal amino acids in CATCH(6K+) and CATCH(6D−) to Qs, increased observed co-assembly kinetics, which also disrupted hierarchical order. Due to the ambient assembly conditions, active CATCH(6K+)-green fluorescent protein fusions could be incorporated into the β-sheet plates and microspheres formed by the CATCH(6K+/6D−) pair, demonstrating the potential to endow functionality.

Introduction

Since the identification of zuotin-derived EAK16-I peptide fibrils in 1993,[1] synthetic peptides that self-assemble into amyloid-like β-sheets have seen increasingly broad use as biomaterials for medical and biotechnology applications.[2] The usefulness of β-sheet-fibrillizing peptides stems from their ability to form biomaterials that span the nano- (e.g., fibrils[3]) to macro-scale (e.g., hydrogels[4]), coupled with their capacity to be imbued with functionality via coupling to other biomolecules (e.g., peptides,[5] proteins,[6] and carbohydrates[7]). Understanding how amino acid sequence characteristics govern β-sheet structure has enabled the design of peptides that spontaneously form biomaterials with predictable architectures at the nanoscale, such as tubes,[8] laminates,[9] and vesicles.[10]

A long-standing challenge is the design of synthetic peptides that spontaneously assemble into β-sheet fibril structures that span longer length scales under ambient conditions (i.e., neutral pH and physiologic ionic strength). Ideally, these synthetic peptides would retain the ability to form multi-scale supramolecular architectures even when coupled to an active biomolecule subunit, such as a folded protein, to endow functionality to the resulting biomaterial. Although multi-scale order can be achieved in assemblies of synthetic peptide-based molecules by manipulating system conditions, for example with heat,[11] pH change,[12] shear,[13] soft lithography,[14] humidity,[15] or applied electric/magnetic fields,[16] the use of these physical and chemical triggers to manipulate the system is likely to damage or degrade sensitive functional biomolecules during the assembly process.

Hierarchical order in natural β-sheet amyloids can occur through different types of inter-fibril contacts, such as "steric zippers"[17] and "electrostatic zippers".[18] The steric zipper is a common motif in synthetic β-sheet peptide design because it depends on short-range van der Waals interactions and hydrophobic collapse that are well behaved in water. In contrast, realizing hierarchical assembly of synthetic β-sheet-forming peptides via electrostatic zippers is rare. For one-peptide systems, the environment generally needs to be manipulated (e.g., highly alkaline or basic pH, organic co-solvent, etc.) to avoid off-pathway kinetic and thermody-

[*] Dr. R. Liu,[+] Dr. D. T. Seroski,[+] Dr. B. Soto Morales, L. Melgar, Prof. G. A. Hudalla
J. Crayton Pruitt Family Department of Biomedical Engineering, University of Florida
Gainesville, FL-32611 (USA)
E-mail: ghudalla@bme.ufl.edu
X. Dong,[+] Prof. C. K. Hall
Department of Chemical and Biomolecular Engineering, North Carolina State University
Raleigh, NC-27695 (USA)
Dr. K. M. Wong, A. S. Robang, Prof. A. K. Paravastu
School of Chemical and Biomolecular Engineering, Georgia Institute of Technology
Atlanta, GA-30332 (USA)
Prof. T. E. Angelini
Department of Mechanical and Aerospace Engineering, University of Florida
Gainesville, FL-32611 (USA)
[+] These authors contributed equally to this work.

© 2023 Wiley-VCH GmbH

namic traps that result from long-range Coulombic interactions.[19] For two-peptide systems, referred to as "co-assemblies", although electrostatic zippers have been reported for an ornithine- and glutamate-rich peptide pair that form β-sheets,[20] as well as a lysine- and glutamate-rich pair,[19] more recent work suggests that hierarchical order via Coulombic interactions favors unstructured peptides, in part because weak intermolecular cohesion allows for rearrangement of oppositely-charged partners within the system.[21]

Although charge-complementary co-assemblies involving peptides and peptide analogs receive significant attention,[22] predicting hierarchical order in these systems is limited by our lack of understanding of how peptide sequence characteristics govern molecular organization. In theory, two different peptides, A and B, could co-assemble into alternating patterns (ABABAB), orthogonal patterns (AAABBB), or in random patterns.[23] In practice, charge-complementary peptide pairs have been shown to generally arrange in an alternating pattern in β-sheets, as would be expected due to electrostatic attraction and repulsion, although deviation from precision is observed.[24] Furthermore, varying the number of charged residues within charge-complementary peptide pairs has been shown to affect the self- versus co-assembly propensity and co-assembly kinetics,[25] while different cationic and anionic peptide pairings yield biomaterials with distinct structural and mechanical properties.[26] These outcomes are empirical. The ability to pick β-sheet fibrillizing peptide pairs that co-assemble into predictable structures *a priori* would establish a new frontier in supramolecular biomaterials.

Here we show that the type of charged amino acid governs hierarchical organization in charge-complementary β-sheet peptide co-assemblies. We studied a set of "CATCH(6X+/6Y−)" peptide pairs (CATCH6X+=Ac-XQXFXFXFXQX-Am, where X=K or R and CATCH6Y-=Ac-YQYFYFYFYQY-Am, where Y=D or E) (Figure 1a) and "CATCH(4K+/4Y−)" peptide pairs (CATCH4K+=Ac-QQKFKFKFKQQ-Am and CATCH4Y-=Ac-QQYFY-FYFYQQ-Am, where Y=D or E) (Figure 4a). We limited this study to only include the amino acids that are employed in ribosome-mediated protein synthesis to allow for creation of functional biomaterials from recombinant CATCH fusion proteins, as well as to the amino acids that can be modeled using the PRIME20 force field.[27] One peptide pair, CATCH(6K+/6D−) formed unique networks of β-sheet-rich plate-like structures in the gel state and β-sheet-rich microspheres in the colloidal solution "sol" state, which were not observed with the other (CATCHX+/Y−) pairs. Simulations suggested that fibrils formed from CATCH(XK+/YD−) pairs had more favorable inter-β-strand interactions and less twist than fibrils formed from CATCH(XK+/YE−) pairs. Experiments also showed glutamic acid increased β-sheet fibril twisting relative to aspartic acid, while arginine increased the observed co-assembly kinetics relative to lysine. Finally, tripartite mixtures of CATCH(6K+), CATCH(6D−), and a CATCH(6K+)-GFP fusion protein yielded fluorescent supramolecular biomaterials, showing that the hierarchical co-assembly behavior of the CATCH(6K+/6D−) pair was robust even in the presence of a much larger folded protein domain. Collectively, this work establishes a basis for understanding how sequence design governs hierarchical order in charge-complementary β-sheet peptide co-assemblies.

Results and Discussion

CATCH(6K+/6D−) co-assemblies have a distinct plate-like morphology in the gel state

CATCH(6R+) and CATCH(6D−) were synthesized using methods previously established for CATCH(6K+) and CATCH(6E−).[28] Like the CATCH(6K+) and CATCH-(6E−) peptides,[25,28] the CATCH(6R+) and CATCH(6D−) peptides were soluble in water up to 12 mM and adopted random coil configurations based on both FTIR measurements and discontinuous molecular dynamics simulations (Figures S1–2). FTIR spectroscopy (Figure S3 and Table S1) and solid-state NMR measurements (Figure S5–6) demonstrated that the peptides in all charge-complementary CATCH(6X+/6Y−) mixtures adopted primarily β-sheet conformations, indicated by peaks centered at $\approx$1620 cm^{-1} in FTIR spectra and right-shifted C_α peaks associated with F, E, K, and D in solid-state NMR spectra. Narrow linewidths in NMR peaks associated with E, K, and D indicated a highly ordered β-sheet structure for the co-assemblies formed by all CATCH(6X+/6Y−) pairs (Figure S5), while integration of the FTIR spectra suggested that pairs including CATCH(6D−) had greater β-sheet content than those including CATCH(6E−) (Table S1).

The identity of the cationic amino acid affected the macro-scale characteristics of equimolar mixtures of CATCH(6X+/6Y−) peptides (Figure 1b). 12 mM mixtures of CATCH(6K+/6D−) and CATCH(6K+/6E−) formed semi-transparent self-supporting macroscopic materials, while CATCH(6R+/6E−) and CATCH(6R+/6D−) formed opaque materials that flowed. These data suggested that replacing K with R in the CATCH(6X+) peptide may alter fibril entanglement or aggregation, while any effect of E versus D in the CATCH(6Y−) peptide was not readily apparent. To further probe the effect of E versus D in the CATCH(6Y−) peptide, we used oscillating rheology to compare the mechanical properties of the macro-scale materials formed by the CATCH(6K+/6D−) pair to those formed by the CATCH(6K+/6E−) pair. Pairs that included CATCH(6R+) were excluded from these studies because they did not form self-supporting materials per the vial inversion test. Aqueous mixtures of CATCH(6K+/6E−) ([total peptide] $\geq$2 mM) have previously been shown to form viscoelastic solids (i.e., gels) that undergo shear-thinning and recovery.[26a] The CATCH(6K+/6D−) pair also formed a viscoelastic solid as indicated by a storage modulus (G′) to loss modulus (G″) ratio (i.e., G′/G″) greater than 1, or equivalently tan(δ) $<$1 (Figure 1c). However, the CATCH(6K+/6D−) gels were significantly stiffer than CATCH(6K+/6E−) gels at an equivalent total peptide concentration, as indicated by the 10-fold greater G′ for the CATCH (6K+/6D+) gels. Like the CATCH(6K+/6E−)

© 2023 Wiley-VCH GmbH

15213773, 2023, 51, Downloaded from https://onlinelibrary.wiley.com/doi/10.1002/anie.202314531 by University Of Florida, Wiley Online Library on [06/08/2024]. See the Terms and Conditions (https://onlinelibrary.wiley.com/terms-and-conditions) on Wiley Online Library for rules of use; OA articles are governed by the applicable Creative Commons License

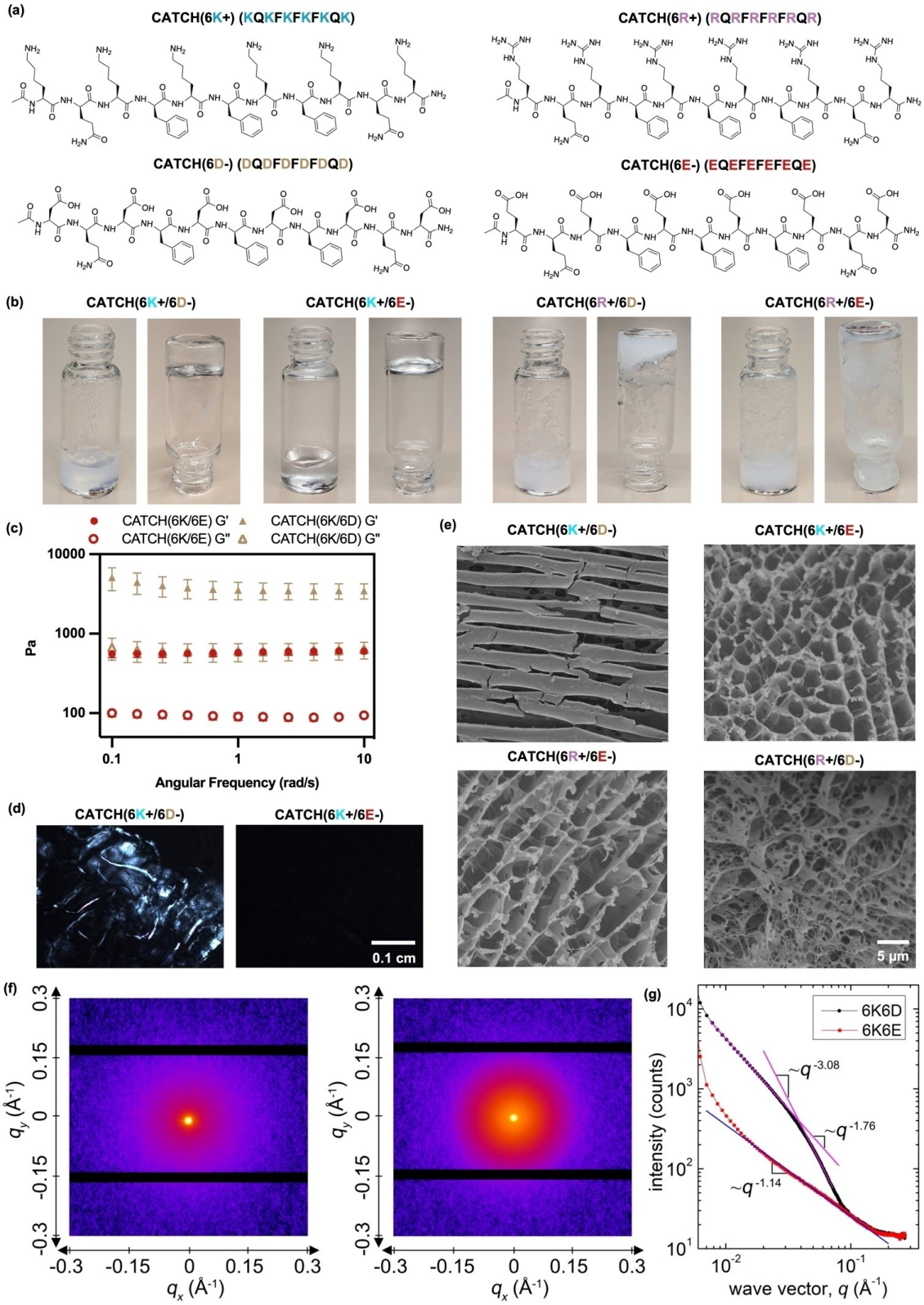

Figure 1. Characterization of the different CATCH(6X+/6Y−) co-assemblies in the gel state. (a) Sequence and chemical structure of the various CATCH(6X+) and CATCH(6Y−) peptides. (b) Inversion test of the different CATCH(6X+/6Y−) pairs at [peptide] = 12 mM in neutral aqueous buffer. (c) G′ and G″ of the materials formed by 12 mM CATCH(6K+/6D−) or CATCH(6K+/6E−) in neutral aqueous buffer at different angular frequencies (mean ± s.d., n = 3). (d) Polarized light micrographs of the materials formed by 12 mM CATCH(6K+/6D−) or CATCH(6K+/6E−). (e) Cryo-SEM images of the materials formed by the different CATCH(6X+/6Y−) pairs at [peptide] = 12 mM in neutral aqueous buffer. Two-dimensional SAXS diffraction pattern (f) and radial intensity profile (g) of the materials formed by 12 mM CATCH(6K+/6D−) or CATCH(6K+/6E−) in neutral aqueous buffer.

© 2023 Wiley-VCH GmbH

15213773, 2023, 51, Downloaded from https://onlinelibrary.wiley.com/doi/10.1002/anie.202314531 by University Of Florida, Wiley Online Library on [06/08/2024]. See the Terms and Conditions (https://onlinelibrary.wiley.com/terms-and-conditions) on Wiley Online Library for rules of use; OA articles are governed by the applicable Creative Commons License

gels reported previously,[26a] the CATCH(6K+/6D−) gels also showed viscoelastic recovery after high-strain (1000 %) disruption; however, CATCH(6K+/6E−) gels showed a greater extent of recovery than CATCH(6K+/6D−) gels over the measurement time frame (Figure S7). The greater stiffness and greater strain sensitivity of CATCH(6K+/6D−) gels relative to the CATCH(6K+/6E−) gels suggested that these two peptide pairs likely formed assemblies with different structural characteristics.

Polarized light microscopy (PLM), scanning electron microscopy (SEM), and small-angle x-ray scattering (SAXS) indicated that the CATCH(6K+/6D−) pair and CATCH(6K+/6E−) pair formed gels with different supramolecular architectures from the nano- to micro-scale. Nematic birefringence was observed when the CATCH(6K+/6D−) gels were viewed between crossed polars, whereas black fields, indicative of no birefringence, were observed for the materials formed by CATCH(6K+/6E−), CATCH(6R+/6E−), and CATCH(6R+/6D−) (Figures 1d and S8). These data suggested that the CATCH(6K+/6D−) gels had an aligned microstructure that lacked positional order at the macro-scale, whereas the materials formed by CATCH(6K+/6E−), CATCH(6R+/6E−), and CATCH(6R+/6D−) were isotropic at the micro-scale. The cloudiness observed in the upright CATCH(6K+/6D−) vial, which was not observed in the CATCH(6K+/6E−) vial (Figure 1b), likely resulted from visible light diffraction due to the aligned microstructure indicated by the PLM images. Consistent with the PLM images, micron-sized plate-like structures and aligned pores were observed in SEM images of gels formed from CATCH(6K+/6D−), whereas more randomly oriented networks of thin fibrils were observed in the gels formed by the CATCH(6K+/6E−) pair, as well as the viscous fluids formed by the CATCH(6R+/6E−) and CATCH(6R+/6D−) pairs (Figures 1e and S9). The thicker fibrillar structures formed by the CATCH(6K+/6D−) pair, coupled with the higher β-sheet content of this pair (Table S1), were consistent with the greater stiffness of CATCH(6K+/6D−) gels relative to CATCH(6K+/6E−) gels.

Isotropic 2D SAXS scattering patterns were observed for both the CATCH(6K+/6D−) and CATCH(6K+/6E−) gels (Figure 1f). Consistent with the PLM micrographs, these scattering patterns indicated that the aligned microstructure observed in SEM images of the CATCH(6K+/6D−) gels did not span the mm-scale. Likewise, the CATCH(6K+/6E−) gels lacked any aligned microstructure. Note that SAXS was not performed on samples of CATCH(6R+/6E−) or CATCH(6R+/6D−) because these materials did not form gels and did not appear to have an aligned microstructure per the PLM and SEM images. To quantitatively search for evidence of micro-scale alignment in the CATCH(6K+/6D−) gels, we integrated the 2D SAXS patterns, $I(q_r,f)$, over finite ranges of q_r, where q_r is the radial distance between any point in the scattering pattern and the origin in q-space, and f is the corresponding azimuthal angle. The resulting plots of $I(f)$ exhibited no significant variations in scattered intensity with direction, consistent with a lack of alignment at the macro-scale (data not shown). However, qualitative differences between CATCH(6K+/6E−) and CATCH(6K+/6D−) samples could be directly seen in the SAXS patterns; CATCH(6K+/6D−) samples generated much stronger scattering at intermediate wave-vectors. To quantitatively analyze this difference, we integrated $I(q_r, f)$ over f, producing plots of $I(q_r)$. When plotted on a log-log scale (Figure 1g), data from the CATCH(6K+/6D+) sample exhibited two different power-law regimes with a crossover at $q \approx 0.039$ Å^{-1}, corresponding to a length-scale of 16.1 nm. In the lower q-range, corresponding to larger length-scales, $I(q_r)$ scaled like $q_r^{-1.76}$; in the higher q-range, corresponding to smaller length-scales, $I(q_r)$ scaled approximately like q_r^{-3}. These two powers and their crossover suggested the presence of an organized plate-like structure in CATCH(6K+/6D−) gels at micrometer length scales, which is larger than a bilayer β-sheet,[29] consistent with the morphology observed in SEM images of CATCH(6K+/6D−) gels. The higher q-range also suggested that CATCH(6K+/6D−) formed more compact structures on scales smaller than the bilayer β-sheet. By contrast, the scattering from CATCH(6K+/6E) samples exhibited no crossover and scaled like $q^{-1.14}$ over a wide range of q-space. This scattering more closely resembled that of randomly oriented rod-like objects, which was generally consistent with the morphology observed in SEM images of CATCH(6K+/6E−) gels. Collectively, the PLM, SEM, and SAXS measurements indicated that the CATCH(6K+/6D−) pair formed hierarchically ordered micro-scale structures that were randomly oriented at the macro-scale in the gel state, whereas the CATCH(6K+/6E−) pair formed fibrillar structures that were disordered at lengths beyond the nano-scale.

The CATCH(6K+/6D−) pair forms β-sheet-rich microspheres in the sol state

A previous report demonstrated that glycosylated β-sheet peptides could form aligned fibrillar networks in both the gel and the sol state, although bundling in the sol state only occurred in the presence of a macromolecular crowder or co-solvent.[30] Here we studied whether CATCH(6K+/6D−) also formed ordered structures in the sol state based on observations that this pair formed unique plate-like structures in the gel state. At a 1 mM concentration, which is below the gel point,[26a] the CATCH(6K+/6D−) peptide pair formed discrete, spherical structures with diameters of 10–200 microns (i.e., "microspheres") that stained positive for the amyloid binding dyes, Thioflavin T (ThT) and Congo Red, suggesting that they w ere rich in β-sheets (Figures 2a and S10–11). Over time, these microspheres tended to cluster, but there was no obvious coalescence as would be expected for phase-separated liquid-like droplets,[31] suggesting that they were instead a solid-like phase (Figure S12). In contrast, at a 1 mM concentration CATCH(6K+/6E−) formed very large ThT-stained aggregates with no discernible structural features, while the CATCH(6R+/6E−) and CATCH(6R+/6D−) pairs formed small ThT-stained flocculates (Figure 2a).

© 2023 Wiley-VCH GmbH

15213773, 2023, 51, Downloaded from https://onlinelibrary.wiley.com/doi/10.1002/anie.202314531 by University Of Florida, Wiley Online Library on [06/08/2024]. See the Terms and Conditions (https://onlinelibrary.wiley.com/terms-and-conditions) on Wiley Online Library for rules of use; OA articles are governed by the applicable Creative Commons License

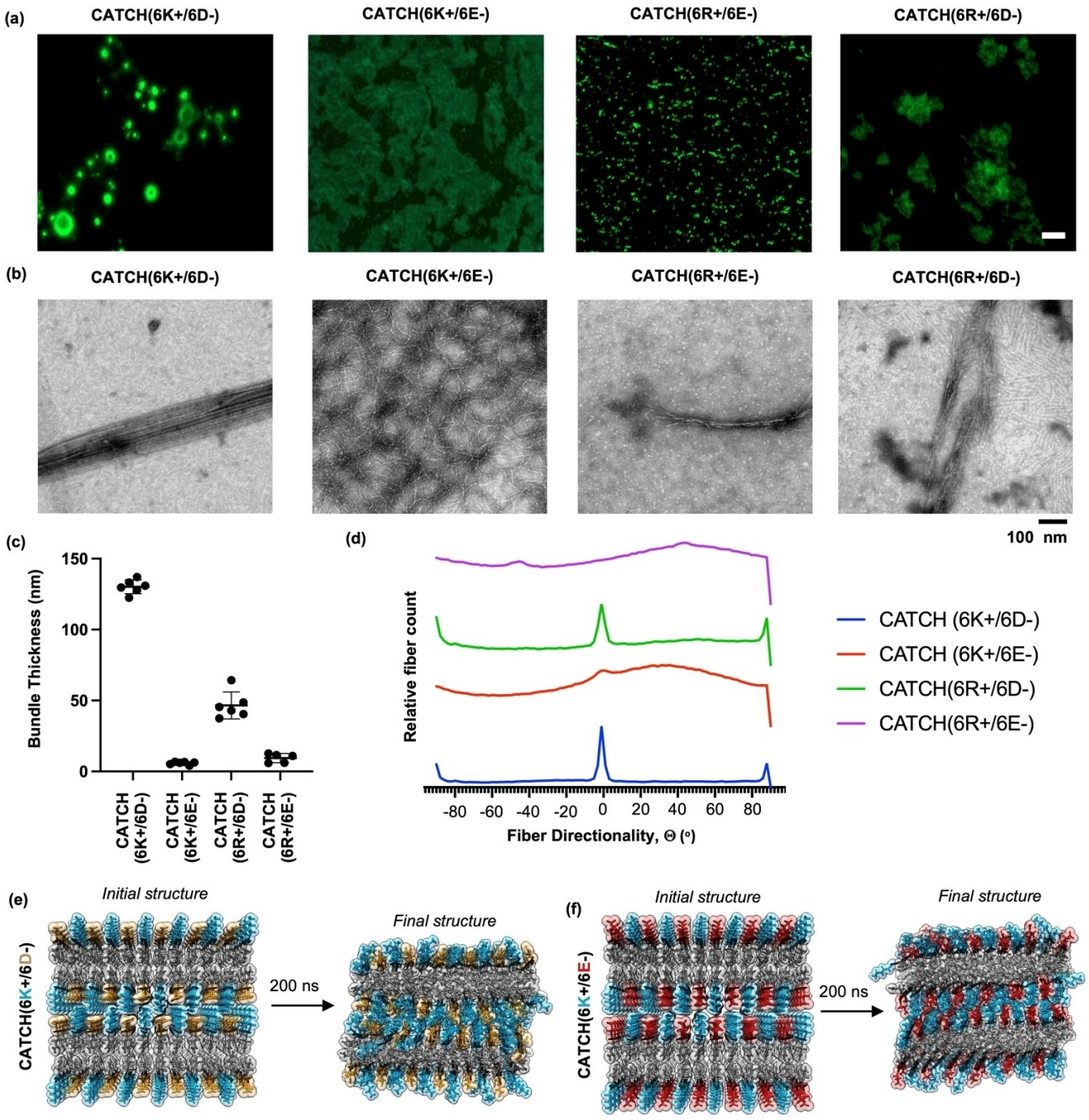

Figure 2. Characterization of the different CATCH(6X+/6Y−) pairs in the sol state. (a) Fluorescence micrographs of the different CATCH(6X+/6Y−) pairs stained with ThT after 60 mins in neutral aqueous buffer at [peptide] = 1 mM. Scale bar = 100 μm. (b) Conventional TEM images of the different CATCH(6X+/6Y−) pairs at [peptide] = 1 mM; (c) Averaged fibril bundle thickness and (d) relative fibril orientation analysis calculated from TEM images. Simulation snapshots of two stacked β-sheet bilayers of (e) CATCH(6K+/6D−) and (f) CATCH(6K+/6E−) at t = 0 and 200 ns.

Conventional TEM identified thick (>100 nm), aligned fibril structures in 1 mM CATCH(6K+/6D−) samples, whereas randomly distributed fibrils with widths of ≈10–20 nm were observed in samples of 1 mM CATCH(6K+/6E−) (Figure 2b). Likewise, in samples of CATCH(6K+/6D−), cryogenic TEM identified regions of aligned fibrils with long persistence lengths and with widths that were comparable to the structures observed with conventional TEM, whereas thinner fibrils with short persistence lengths and a more isotropic distribution were observed in samples of CATCH(6K+/6E−) (Figure S13). Some twisted multilayer structures were observed in conventional TEM images of mixtures of CATCH(6R+/6D−) and CATCH(6R+/6E−) (Figure 2b), but these bundles were thinner than those formed by CATCH(6K+/6D−) (Figure 2c). We note that some protofibrils or other non-fibrillar aggregates (i.e., oblong and round white features) are sometimes found in conventional TEM images for CATCH(6K+/6D−),

© 2023 Wiley-VCH GmbH

15213773, 2023, 51, Downloaded from https://onlinelibrary.wiley.com/doi/10.1002/anie.202314531 by University Of Florida, Wiley Online Library on [06/08/2024]. See the Terms and Conditions (https://onlinelibrary.wiley.com/terms-and-conditions) on Wiley Online Library for rules of use; OA articles are governed by the applicable Creative Commons License

CATCH(6R+/6D−), and CATCH(6R+/6E−); the high density of thin fibrils on the CATCH(6K+/6E−) sample grid may have occluded observation of these structures in this sample or they may not exist.

Quantitative analysis of fibril orientation, Θ, showed that mixtures including CATCH(6D−) had greater alignment than mixtures including CATCH(6E−), with CATCH(6K+/6D−) having the highest degree of alignment (Figure 2d). Atomistic simulations of idealized hypothetical β-sheet bilayers with an alternating +/− β-strand configuration predicted that stacked bilayers of CATCH(6K+/6D−) co-assemblies would have greater van der Waals (VDW) and electrostatic (ELE) interactions between the charged amino acids that reside between the bilayers than stacked CATCH(6K+/6E−) bilayers (Figures 2e–f, Table S2). Consistent with these simulations, analysis of the FTIR spectra identified a strong peak centered at $\approx$1550 cm^{-1} in the CATCH(6K+/6D−) spectrum that was red-shifted relative to the ionized aspartic acid (COO−) side-chain peak centered $\approx$1570 cm^{-1} observed in the spectrum of CATCH-(6D−) alone (Figure S4). In contrast, the glutamic acid (COO−) side chain peak was centered at the same wavenumber and had similar intensity in the spectra of CATCH(6K+/6E−) and CATCH(6E−) alone (Figure S4). The emergence of the stronger, red-shifted peak in the CATCH(6K+/6D−) FTIR spectrum is associated with salt-bridge formation.[32]

Measuring the distance between the backbone atoms on the 2nd and 3rd layers in the stacked bilayers suggested that CATCH(6K+/6D−) β-sheets would stack 2 Å closer together than CATCH(6K+/6E−) β-sheets (Table S3). Notably, this was consistent with the higher *q*-range SAXS measurements (Figure 1g), which suggested that mixtures of CATCH(6K+/6D−) formed more compact structures than CATCH(6K+/6E−) in the gel state.

We noted from the TEM images that the fibrils formed from pairs that included CATCH(6E−) appeared to have a shorter twist pitch than fibrils formed from pairs that included CATCH(6D−), which tended to be less twisted. Consistent with this, atomistic simulations predicted that a CATCH(6K+/6D−) bilayer or multilayer would have a flatter conformation than a CATCH(6K+/6E−) bilayer or multilayer (Figures 2e–f, Figure S14); this is because the angle between neighboring peptides in CATCH(6K+/6D−) β-sheets is predicted to be smaller than in CATCH(6K+/6E−) β-sheets (−2.22° and −3.55°, respectively) (Table S4). Consistent with this, the β-sheet amide I peak in the FTIR spectrum for CATCH(6K+/6D−) was red-shifted to 1617 cm^{-1} relative to the β-sheet amide I peak in the FTIR spectrum for CATCH(6K+/6E−) (1619 cm^{-1}) (Figure S3), which can be attributed to a flatter β-sheet morphology.[33] Taken together with the TEM images and their analysis (Figure 2b–d), these data suggested that the CATCH(6D−) peptide favored the formation of fibrils with a shallow pitch and a greater degree of stacking than fibrils formed with the CATCH(6E−) peptide, which had a greater twist and underwent lesser stacking.

CATCH(6K+/6D−) co-assembled with slower kinetics than the other CATCH(6X+/6Y−) pairs

Prior reports have demonstrated that the kinetics of β-sheet fibril assembly depend on the aggregation mechanism,[34] which can influence the final structure of the assembled materials.[35] The secondary structures adopted by the peptides in the various CATCH(6X+/6Y−) mixtures differed over time in the sol state (Figure 3). Circular dichroism measurements demonstrated that all the different CATCH peptides were in random coil conformations when alone in a neutral aqueous buffer (Figure S15), consistent with FTIR measurements and simulations of these peptides at higher concentrations. The peptides in the CATCH(6K+/6D−) mixture were primarily in random coil conformations immediately after combining them and underwent structural transition over time, as indicated by the emergence of a single strong minimum between 205–210 nm (Figure 3a–b). This minimum was inconsistent with a typical β-sheet or random coil signature, but instead was similar to spectra reported for large anisotropic fibrillar structures, such as collagen type I fibers.[36] We infer that this spectrum reflects the thick fibril bundles observed in the TEM images of the CATCH(6K+/6D−) pair in the sol state as shown in Figure 2b. Peptides in the CATCH(6K+/6E−) mixture existed in a combination of random coil and β-sheet conformations when measured immediately after combining them and underwent a structural transition into a predominantly β-sheet conformation over time, consistent with a prior report (Figure 3c–d).[28] Notably, peptides in mixtures that included CATCH(6R+) were predominantly in a β-sheet conformation immediately after mixing, indicated by strong ellipticity minima between 215–220 nm (Figure S16). While the CD spectrum of the CATCH(6R+/6E−) mixture was largely unchanged over time, the minimum and maximum for the CATCH(6R+/6D−) mixture red-shifted by $\approx$10 nm (Figure S17). This suggested that the CATCH(6R+/6D−) peptides and/or fibrils underwent some structural transition, possibly the formation of the multi-layer structures observed in TEM images. Recall that FTIR and NMR measurements indicated that all CATCH(6X+/6Y−) mixtures were also rich in β-sheets in the gel state (Figures S3, S5, S6, and Table S1).

Consistent with the CD measurements, ThT fluorimetry measurements also indicated that the co-assembly kinetics differed for the different CATCH(6X+/6Y−) pairs (Figure 3e). In particular, the kinetic profile for the 1 mM CATCH(6K+/6D−) mixture had a discernible lag phase that was not seen for the other pairs, followed by a slower growth profile that began to plateau by $\approx$1 h. In contrast, pairs that included CATCH(6R+) plateaued within seconds to minutes, while the CATCH(6K+/6E−) pair plateaued by $\approx$10 min. After 1 h, the 1 mM CATCH(6K+/6D−) pair had the highest total ThT signal (Figure S18). At 120 h, by which point the CATCH(6K+/6D−) and CATCH(6K+/6E−) pairs reached equilibrium, the CATCH(6K+/6D−) pair had a higher maximum ThT signal than the CATCH(6K+/6E−) pair at all concentrations tested (Figure 3f and S19). However, the CATCH(6K+/6D−) and CATCH(6K+

© 2023 Wiley-VCH GmbH

15213773, 2023, 51, Downloaded from https://onlinelibrary.wiley.com/doi/10.1002/anie.202314531 by University Of Florida, Wiley Online Library on [06/08/2024]. See the Terms and Conditions (https://onlinelibrary.wiley.com/terms-and-conditions) on Wiley Online Library for rules of use; OA articles are governed by the applicable Creative Commons License

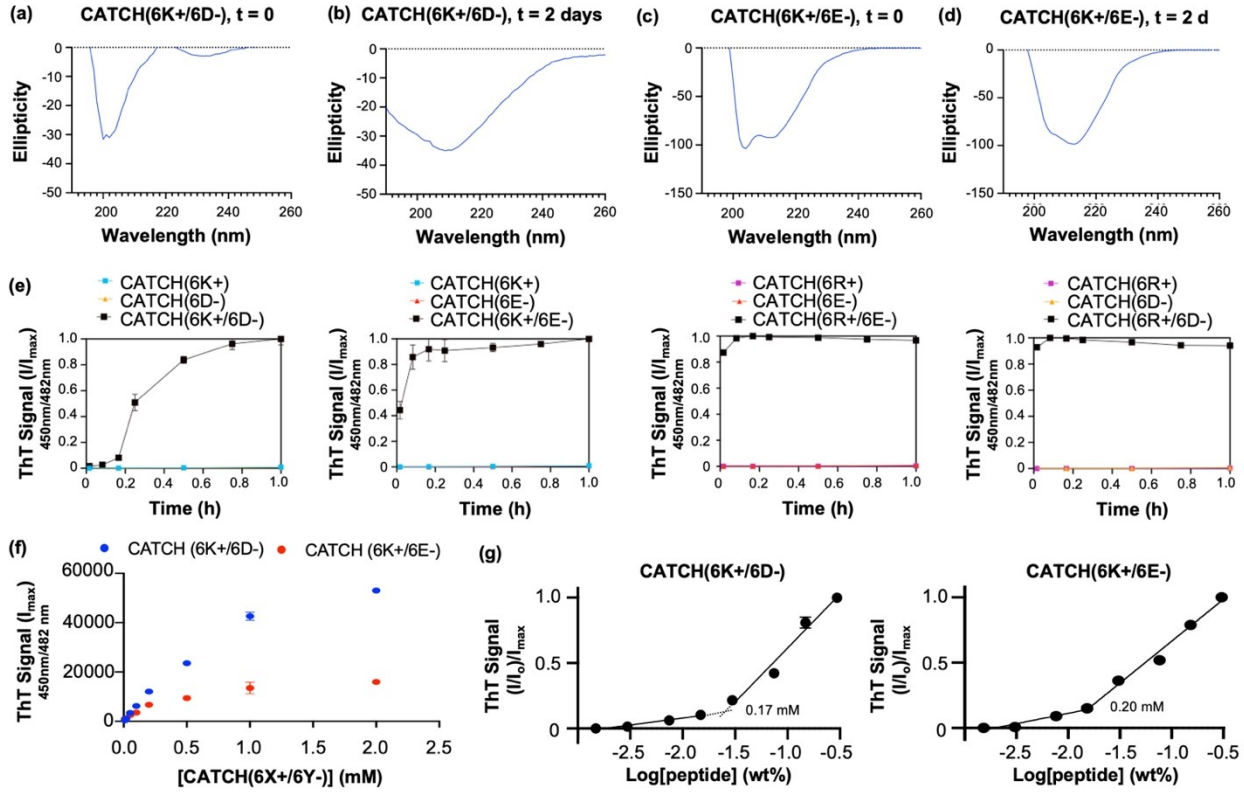

Figure 3. Co-assembly kinetics of the different CATCH(6X+/6Y−) peptide pairs. (a-d) CD spectra of 125 μM CATCH(6K+/6D−) or CATCH(6K+/6E−) in neutral aqueous buffer immediately after mixing (i.e., "t=0") and after 2 days at RT; (e) Co-assembly kinetics profiles of the different CATCH(6X+/6Y−) pairs at [peptide]=1 mM measured via ThT fluorimetry (mean + s.d., n=3); (f) Maximum ThT fluorescence versus [peptide] and (g) critical fibrillization concentration and for the CATCH(6K+/6D−) and CATCH(6K+/6E−) pairs.

/6E−) pairs showed similar concentration-dependent behavior with regard to fibril growth (Figure 3g). In particular, the critical concentrations for fibril growth for CATCH(6K+/6E−) and CATCH(6K+/6D−) were ≈0.20 and 0.17 mM, respectively. This was consistent with prior CD measurements, which showed that peptides in CATCH(6K+/6E−) mixtures underwent a transition from a combination of random coil and β-sheet conformations to predominantly β-sheet conformations over the range of 125–300 μM.[28]

Mutating the hydrophilic face disrupts the micro-scale co-assembly of CATCH(6K+/6D−)

The data presented in Figures 1–2 demonstrate that the CATCH(6K+/6D−) peptide pair forms unique supramolecular architectures, including β-sheet-rich plates and β-sheet-rich microspheres, which are not seen with the other CATCH(6X+/6Y−) pairs. Informed by simulations, we expected that peptide designs providing weaker interfacial contacts would disrupt hierarchical co-assembly. To test this hypothesis, we studied the co-assembly of the CATCH(4X+/4Y−) variants (Figure 4a), which have fewer charged residues than the CATCH(6X+/6Y−) pairs, and thus should have a weakened electrostatic zipper.

Like the CATCH(4E−) peptide reported previously,[26a] the CATCH(4D−) peptide was soluble in water up to 12 mM, adopted random-coil configurations when alone, and formed a β-sheet-rich structure when in an equimolar mixture with the CATCH(4K+) peptide (Figure S20). ThT fluorimetry indicated that the CATCH(4K+/4D−) and CATCH(4K+/4E−) pairs had similar critical fibrillization concentrations (0.17 and 0.2 mM, respectively) (Figure S21), which were comparable to the critical fibrillization concentrations of the CATCH(6K+/6D−) and CATCH(6K+/6E−) pairs (Figure 3g). Thus, the difference in number of charged residues did not affect the fibrillization threshold. ThT fluorimetry also suggested that the CATCH(4K+/4D−) pair formed more fibril mass than the CATCH(4K+/4E−) pair (Figure S22), consistent with the relationship between the CATCH(6K+/6D−) and CATCH(6K+/6E−) pairs (Figure 3f). However, while CATCH(4K+/4E−) demonstrated a similar kinetic profile as the CATCH(6K+/6E−) pair (Figure 4b and Figure 3e, respectively), the CATCH(4K+/4D−) pair demonstrated no lag phase and much faster co-assembly kinetics than the CATCH(6K+/6D−) pair (Figure 4b and Figure 3e, respectively). Thus, despite sharing the ability to form β-sheets upon mixing, the CATCH(6K+/6D−) and CATCH(4K+/4D−) pairs showed different co-assembly behaviors.

© 2023 Wiley-VCH GmbH

15213773, 2023, 51, Downloaded from https://onlinelibrary.wiley.com/doi/10.1002/anie.202314531 by University Of Florida, Wiley Online Library on [06/08/2024]. See the Terms and Conditions (https://onlinelibrary.wiley.com/terms-and-conditions) on Wiley Online Library for rules of use; OA articles are governed by the applicable Creative Commons License

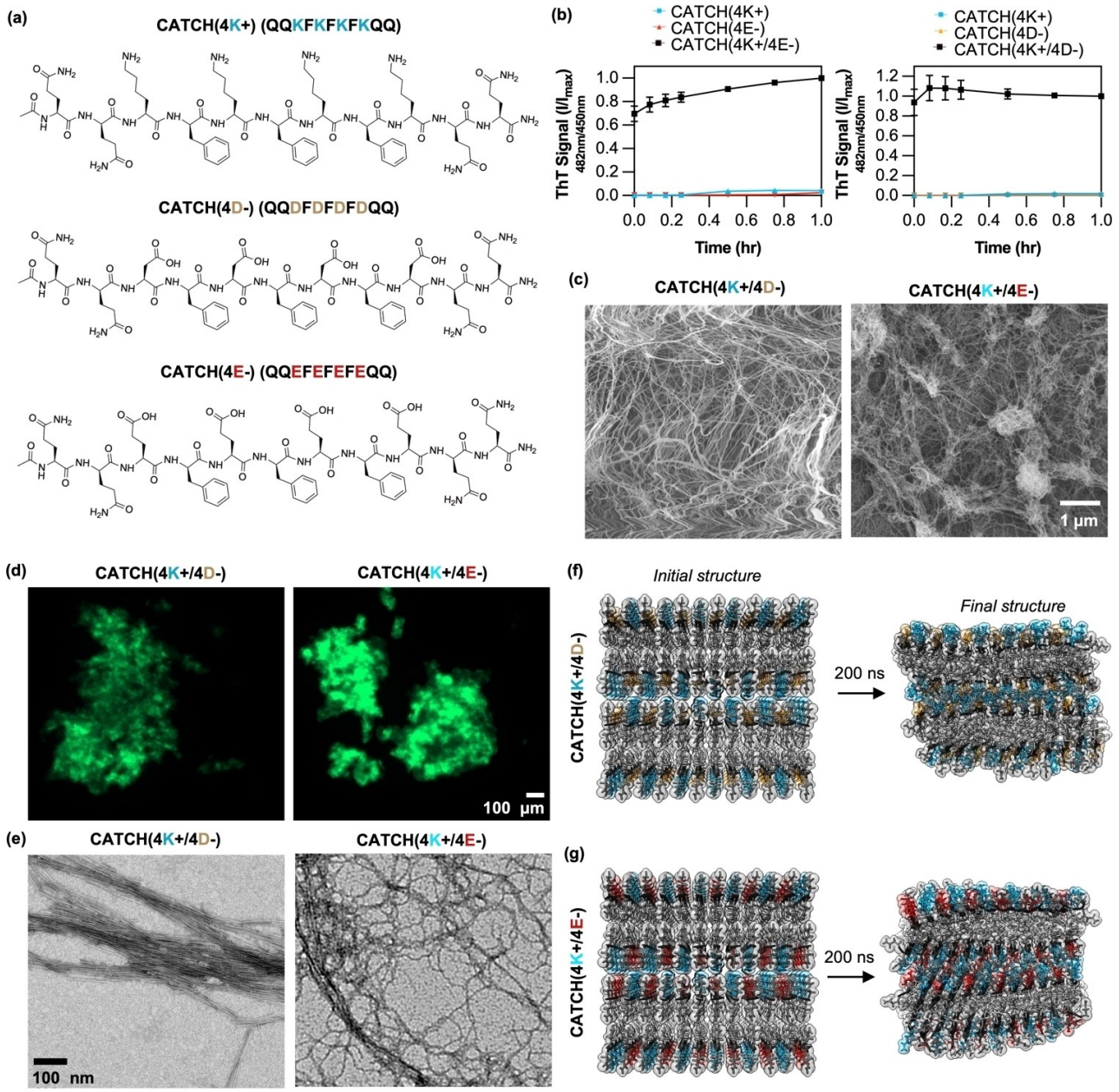

Figure 4. Characterization of CATCH(4K+/4Y−) co-assemblies in the gel and sol state. (a) Sequence and chemical structure of the various CATCH(4X+) and CATCH(4Y−) peptides; (b) Co-assembly kinetics profiles of the different CATCH(4X+/4Y−) pairs at [peptide] = 1 mM measured via ThT fluorimetry (mean + s.d., $n = 3$); (c) Conventional SEM images of the materials formed by the CATCH(4K+/4D−) and CATCH(4K+/4E−) pairs at [peptide] = 12 mM in neutral aqueous buffer. (d) ThT fluorescence micrographs and (e) conventional TEM images of the materials formed by the CATCH(4K+/4D−) and CATCH(4K+/4E−) pairs at [peptide] = 1 mM in neutral aqueous buffer. Simulation snapshots of two stacked β-sheet bilayers of (f) CATCH(4K+/4D−) and (g) CATCH(4K+/4E−) at t = 0 and 200 ns.

Differences in the co-assembly behavior of the CATCH(4K+/4D−) pair relative to the CATCH(6K+/6D−) pair correlated with differences in supramolecular morphology. In particular, conventional SEM of the CATCH(4K+/4D−) pair identified a network of isotropic nanofibers in the gel state (Figure 4c), which differed considerably from the large plates seen in gels formed by the CATCH(6K+/6D−) pair (Figure 1e). Instead, the architecture of the network formed by the CATCH(4K+/4D−) pair resembled the networks formed by the CATCH(4K+/4E−) pair and the CATCH(6K+/6E−) pair in the gel state (Figures 4c and 1e, respectively). Likewise, in the sol state, the CATCH(4K+/4D−) pair formed large aggregates with no discernible structural characteristics (Figure 4d), which were morphologically different than the microspheres formed by the CATCH(6K+/6D−) pair under identical conditions (Figure 2a). In conventional TEM images, CATCH(4K+/4D−) co-assemblies appeared as

© 2023 Wiley-VCH GmbH

15213773, 2023, 51, Downloaded from https://onlinelibrary.wiley.com/doi/10.1002/anie.202314531 by University Of Florida, Wiley Online Library on [06/08/2024]. See the Terms and Conditions (https://onlinelibrary.wiley.com/terms-and-conditions) on Wiley Online Library for rules of use; OA articles are governed by the applicable Creative Commons License

relatively flat fibrils (i.e., had a shallow pitch twist) with a long persistence length that had some tendency to laterally associate (Figure 4e). But, the CATCH(4K+/4D−) co-assemblies lacked the long-range order seen for the CATCH(6K+/6D−) pair, which persisted over the entire micrograph viewing area (>1 μM) (Figure 2b).

Atomistic simulations predicted that CATCH(4K+/4D−) fibrils would have a shallower pitch twist (i.e., would be flatter) than CATCH(4K+/4E−) fibrils (Figure 4f, g and Figure S14, Table S4). Likewise, atomistic simulations predicted that CATCH(4K+/4D−) multilayers would stack closer together than CATCH(4K+/4E−) multilayer (Table S3). Thus, CATCH(4K+/4D−) fibrils were expected to share morphological similarities with the CATCH(6K+/6D−) fibrils, while CATCH(4K+/4E−) fibrils were expected to share morphological similarties with the CATCH(6K+/6E−) fibrils; these relationships were also reflected in the conventional TEM images of these various CATCH(X+/Y−) pairs. Unexpectedly, though, atomistic simulations predicted that the interface between bilayers in a CATCH(4K+/4D−) multilayer stack would have comparable van der Waals and electrostatic interactions to CATCH(6K+/6D−) stacks, which were greater than the interaction energies between CATCH(4K+/4E−) or CATCH(6K+/6E−) stacks (Table S2). Thus, despite being longer than aspartic acid by one methylene, the glutamine residues at the termini of CATCH(4K+) and CATCH-(4D−) did not sterically occlude electrostatic zipper formation. Furthermore, reducing the number of charged residues from 6 to 4 did not necessarily weaken the interfibril electrostatic zipper in a stack of CATCH(X+/Y−) bilayers as we had expected. This raised questions as to why the CATCH(4K+/4D−) system did not form the β-sheet-rich microspheres and β-sheet-rich micron-sized plates observed with the CATCH(6K+/6D−) system. The faster co-assembly kinetics for the CATCH(4K+/4D−) pair (Figure 4b) suggested that this system is dominated by favorable primary nucleation events, whereas the lag phase observed for CATCH(6K+/6D−) co-assembly suggests a role for both primary (i.e., in solution) and secondary (i.e., on fibril) nucleation events. Thus, CATCH(4K+/4D−) fibrils that emerge rapidly may undergo lateral association into furcated structures, analogous to the mechanism of dichotomous coalescence proposed for mouse prion protein fibrillization.[37] In contrast, CATCH(6K+/6D−) may follow a pathway of slower primary nucleation followed by attached lateral nucleation that leads to thickening, as seen for insulin fibril growth;[38] notably, the formation of insulin spherulites, which share morphological similarities with the CATCH(6K+/6D−) microspheres reported here, also depends on attached lateral nucleation but is followed by branching instead of thickening.[39] We posit that a hierarchical growth process dependent on attached lateral nucleation would explain, at least in part, the diminished recovery of CATCH(6K+/6D−) gel stiffness after high-strain disruption, given that the applied strain would be unlikely to completely dissassemble the peptides (i.e., return them to their initial random coil monomeric state). Rather, high-strain would likely lead to fracture of the micron-scale plate-like structures into fragments with a slowed re-assembly time due to a relatively slow rate of diffusion.[40]

A CATCH-protein fusion can be incorporated into CATCH(6K+/6D−) microscopic plates and microspheres

While the formation of unique microscopic biomaterials by the CATCH(6K+/6D−) pair is interesting, these materials will ultimately only be useful for medical or biotechnology applications if they can be functionalized while maintaining the underlying supramolecular structural characteristics. We previously reported that fusing the CATCH(6E−) peptide onto the terminus of green fluorescent protein (GFP) enabled stable integration of the active protein into CATCH(4K+/6E−) hydrogels.[28] Here we show that GFP can also be integrated into hierarchically-ordered sol and gel state co-assemblies of CATCH(6K+/6D−). We first created a new fusion protein consisting of CATCH(6K+) linked to GFP, referred to as CATCH(6K+)-GFP (Figure S23). A ternary mixture of CATCH(6K+), CATCH(6K+)-GFP, and CATCH(6D−) formed a fluorescent self-supporting gel (Figure 5a), which had a microscopic plate-like network architecture when viewed with cryo-SEM (Figure 5b). CATCH(6K+)-GFP also integrated into the microspheres formed by a ternary mixture of CATCH(6K+), CATCH-(6K+)-GFP, and CATCH(6D−) in the sol state (Figure 5c). These microspheres bound Congo Red (Figure 5d), suggesting that the presence of the GFP domain did not disrupt β-

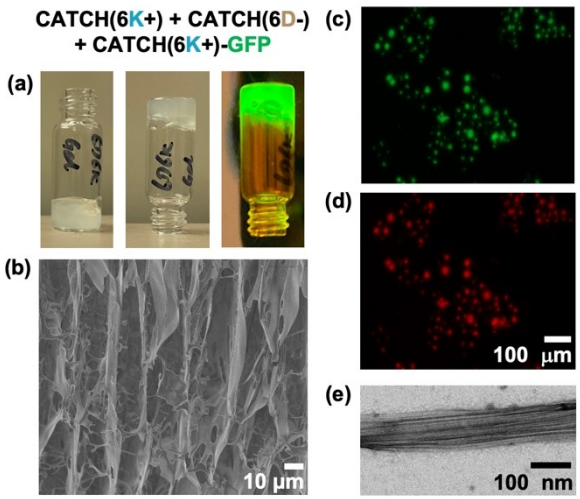

Figure 5. A functional protein domain can be integrated into CATCH(6K+/6D−) co-assemblies. (a) Digital images of the inversion test and green fluorescence emitted by a gel formed by a ternary mixture of 12 mM CATCH(6K+/6D−) and 1 μM CATCH(6K+)-sfGFP. (b) Cryo-SEM image of a gel formed by a ternary mixture of 12 mM CATCH(6K+/6D−) and 1 μM CATCH(6K+)-sfGFP. (c) GFP and (d) Congo Red fluorescence micrographs of the microspheres formed in a ternary mixture of 1 mM CATCH(6K+/6D−) and 1 μM CATCH(6K+)-sfGFP. (e) Conventional TEM image of the stacked β-sheet structure formed in a ternary mixture of 1 mM CATCH(6K+/6D−) and 1 μM CATCH(6K+)-sfGFP.

© 2023 Wiley-VCH GmbH

15213773, 2023, 51, Downloaded from https://onlinelibrary.wiley.com/doi/10.1002/anie.202314531 by University Of Florida, Wiley Online Library on [06/08/2024]. See the Terms and Conditions (https://onlinelibrary.wiley.com/terms-and-conditions) on Wiley Online Library for rules of use; OA articles are governed by the applicable Creative Commons License

sheet formation or the inter-fibril interactions that were required for microsphere formation. Further supporting the ThT micrographs, conventional TEM identified thick, aligned bundles with striations (Figure 5e), indicative of the presence of multiple stacked fibril layers in the ternary mixture of CATCH(6K+), CATCH(6K+)-GFP, and CATCH(6D−) in the sol state. Together, these data demonstrated that the unique biomaterials formed by the CATCH(6K+/6D−) peptide pair were amenable to functionalization with a bulky protein domain, without sacrificing hierarchical order or protein activity.

Discussion

The data presented here demonstrate that the CATCH(6K+/6D−) pair undergoes concentration-dependent co-assembly into β-sheet-rich microspheres or β-sheet-rich gels with a micron-scale plate-like morphology that are not seen with other CATCH(X+/Y−) pairs. Although tens of synthetic peptides that assemble into β-sheet fibrils have been reported,[41] only a handful of examples of synthetic β-sheet multilayers exist. Instead, recent reports suggest that β-sheet formation may impede hierarchical co-assembly across length scales because strong intermolecular cohesion between β-strands prevents molecular rearrangement.[21a,b] Our report shows that hierarchical order can be realized in charge-complementary β-sheet peptide co-assemblies, as was reported previously for a glutamate- and ornithine-rich peptide pair,[20] but it is not ubiquitous. Rather, the charged amino acid side-chain chemistry governs hierarchical order.

In peptide fibrillization, β-sheet layers (i.e., "tapes") form via hydrogen bonding between the amide backbones of peptides in an extended β-strand conformation, while stacking of the β-sheets results from interactions between the amino acid side chains of peptides in adjacent layers.[42] Generally, the extended β-strand conformation results in the presentation of neighboring amino acid side chains on the opposite sides of the peptide backbone and, in turn, on opposite faces of the tape. Designing hydrophobic steric zippers onto one face of a tape to favor bilayer formation is relatively simple; an alternating sequence of hydrophobic and hydrophilic amino acids will generally suffice. It is the designing-in of sites of molecular recognition onto the hydrophilic "wet" faces of the tapes to drive stacking that poses a challenge. This is because (1) interfacial interactions that are too weak will limit lamination,[40] and (2) the twisting of β-sheets, which is often associated with amino acid chirality, can impose a physical constraint on the number of possible laminated layers due to the unfavorable energy associated with tape tilting and bond bending.[43] Indeed, examples of multilayered β-sheet laminates have generally employed peptides with both D- and L- amino acids or charged side chains to disfavor tape twisting.[9a,19, 44] The results presented here suggest that a high density of charged residues on the "wet" face of a β-sheet bilayer does not universally provide an electrostatic zipper capable of mediating hierarchical assembly over multiple length scales. Instead, the side-chain chemistry of the charged amino acids dictates CATCH(X+/Y−) pair co-assembly kinetics and fibril morphology, which collectively govern the propensity for β-sheet stacking. For example, the CATCH(XK+/YE−) pairs failed to form multilayer structures due to both (1) weaker interfacial interactions, as predicted from simulations, and (2) increased β-sheet twisting, as predicted from simulations and seen experimentally.

In general, we observed an inverse relationship between co-assembly kinetics and hierarchical order in CATCH(X+/Y−) systems. CD spectroscopy and ThT fluorimetry demonstrated that co-assembly proceeded faster in mixtures that included the CATCH(6R+) peptide when compared to mixtures that included CATCH(6K+). The increased co-assembly rate in CATCH(6R+) mixtures likely reflects increased long-range Coulombic attraction due to differences in the guanidinium group of the arginine side-chain versus the amine of the lysine side chain; the former has a higher pKa and can form electrostatic interactions in more possible directions. Mixtures that included CATCH(6R+) also failed to form self-supporting gels. These observations suggest that highly favorable primary nucleation in mixtures that contain the CATCH(6R+) peptide may limit the extent of both β-sheet elongation and β-sheet stacking, ultimately leading to fibril structures that are unable to form either a physically entangled gel or a hierarchically-ordered structure.

However, the chemical identity of the CATCH(6Y−) peptide also affected the rate and extent of co-assembly. CATCH(6K+/6D−) mixtures showed a pronounced lag phase and a higher maximum ThT signal than CATCH(6K+/6E−) mixtures. Given that CATCH(6K+), CATCH(6D−), and CATCH(6E−) all have similar chemical structures, the higher maximum ThT signal suggested that CATCH(6K+/6D−) mixtures may yield more fibril mass than CATCH(6K+/6E−) at equilibrium. We postulate that a difference in the extent of fibril formation could result from differences in the mechanism of co-assembly of the CATCH(6K+/6D−) pair versus the CATCH(6K+/6E−) pair. One could envision that for CATCH(6K+/6E−), increases in fibril mass would only result from growth along the long axis of β-sheet bilayers due to addition of free peptides onto the chain ends (i.e., 1D growth). Once the free peptide concentration decreases below the critical concentration for nucleation, no new fibrils would form. Instead, fibril mass could only increase via addition of peptides onto the chain end, the extent of which would be limited by the dissociation constant of the free peptide for the chain end. In contrast, in CATCH(6K+/6D−) mixtures, increases in fibril mass could result from either elongation via addition of free peptides onto the bilayer chain ends, or through stacking of charge-complementary free peptides onto the charged face of the bilayer (i.e., 2D growth). We note that this mechanism bears resemblance to the secondary nucleation pathway referred to as attached lateral nucleation and thickening.[45] Such 2D growth would be less restricted when free peptide remains available in the system because the addition of any peptide onto the growing structure would re-introduce a new "reactive surface" onto which an additional peptide molecule could attach. Impor-

© 2023 Wiley-VCH GmbH

15213773, 2023, 51, Downloaded from https://onlinelibrary.wiley.com/doi/10.1002/anie.202314531 by University Of Florida, Wiley Online Library on [06/08/2024]. See the Terms and Conditions (https://onlinelibrary.wiley.com/terms-and-conditions) on Wiley Online Library for rules of use; OA articles are governed by the applicable Creative Commons License

tantly, the unique lag phase observed in the kinetic profiles of CATCH(6K+/6D−) mixtures suggests that primary nucleation was the rate-limiting step of the assembly process for this system, but not for the other CATCH(X+/Y−) systems. Thus, the charged amino acids influence hierarchical co-assembly by way of the effects of electrostatic interactions on co-assembly kinetics.

Interestingly, the lag phase observed in the kinetic profiles of CATCH(6K+/6D−) mixtures has not been observed with other CATCH peptide pairs reported to date. Computational models included in a complementary study suggest this may be due to a weaker tendency of CATCH(6D−) to form an α-helix when compared to CATCH(6E−);[46] the α-helix has been reported to have a greater propensity for conversion to a β-strand than the random coil.[47] Our computational prediction was surprising in light of prior studies which suggested that an N-terminal aspartic acid has greater helix-inducing activity than an N-terminal glutamic acid,[48] from which one would expect more helicity for CATCH(6D−) than CATCH(6E−). Likewise, N-terminal glutamine, as exists on CATCH(4D−), is suggested to be a poor helix-stabilizing residue.[49] yet the CATCH(4K+/4D−) pair demonstrated faster co-assembly kinetics than the CATCH(6K+/6D−) pair. One important consideration is that N-terminal acetylation, such as that on the CATCH peptides, has also been shown to counteract some of the effects of the N-terminal amino acid on helicity.[49] Collectively, this suggests that amino acids at other positions within the CATCH(6Y−) peptides contribute to their relative helicities. Alternatively, the observed differences in CATCH(6K+/6D−) versus CATCH(6K+/6E−) kinetics may be due to the tendencies of D and E to interact with ions present in solution. Recent computational and experimental work has shown that D-rich peptides interact with ions, such as chloride and calcium, to a greater extent than E-rich peptides.[50] Thus, one can envision that greater charge-shielding of CATCH(6D−) in the phosphate-buffered saline used in these studies may reduce its electrostatic attraction for CATCH(6K+) or sterically inhibit CATCH(6D−) association with the ends or surfaces of growing CATCH β-sheets, either of which would be expected to decrease the rate of co-assembly. Again, though, the unusual kinetic behavior of the CATCH(6K+/6D−) pair relative to CATCH(4K+/4D−) highlights the need for continued inquiry into the complicated relationships between amino acid content and synthetic β-sheet fibril structure.

Finally, in addition to kinetics, TEM images, SAXS measurements, and computational models suggested that the identity of the charged amino acid also influenced the morphology of CATCH β-sheet fibrils. Fibrils formed by the CATCH(6K+/6D−) and CATCH(4K+/4D−) pairs tended to have more compact structures than those formed by the CATCH(6K+/6E−) and CATCH(4K+/4E−) pairs. Fibrils formed by pairs that included CATCH(6D−) or CATCH(4D−) also tended to have a longer pitch along their contour length than those formed by pairs that included CATCH(6E−) or CATCH(4E−). Prior reports have demonstrated that a shorter pitch tends to lead to a decrease in the number of stacked β-sheet layers due to the energetic penalties associated with tape tilting and bond bending,[51] while fibril helical symmetry has been suggested to weaken the inter-layer hydrogen bond strength as the number of layers increases.[52] Recent work suggests that fibril pitch is also governed by electrostatic energy, where stronger interactions lead to a smaller pitch; ions present in solution can reduce this electrostatic energy, leading to fibrils with a longer pitch.[53] We infer from this that CATCH(XK+/XE−) fibrils have greater intra- β-sheet electrostatic interactions than CATCH(XK+/XD−) fibrils. This may result from (1) the additional methylene in the E side-chain, which has a comparable length to the K side-chain, (2) the higher ion-binding potential of D-rich peptides when compared to E-rich peptides, or (3) both. Thus, interactions between CATCH(6D−) peptides and ions in solution may alter both the co-assembly kinetics and fibril structure, which together facilitate the hierarchical organization of CATCH(6D−) and CATCH(6K+) into materials with multi-scale structural order in water at physiologic pH and ionic strength.

Conclusion

This report demonstrated the effects of the charged amino acid type on the hierarchical order of CATCH(X+/Y−) co-assemblies. A new peptide pair, CATCH(6K+/6D−), demonstrated concentration-dependent formation of hierarchically-ordered microscopic biomaterials. This hierarchical order could be disrupted by replacing D with E, which increased fibril twisting, replacing K with R, which increased observed co-assembly kinetics, or replacing the charged N- and C-terminal residues with Qs. This work establishes a molecular basis for predicting the unguided co-assembly of charge-complementary synthetic β-sheet-forming peptide pairs into functional biomaterials with structural order spanning length scales.

Acknowledgements

This research was supported by the National Science Foundation (RAISE 1743432 and OAC1931430). This work was also partially supported by the National Institute on Aging of the National Institutes of Health and the National Institute on Minority Health and Health Disparities (award number RF1AG073434-01A1 to A.K.P.). We would also like to thank Karen Kelley, Paul Chipman, Kimberly Backer-Kelley, and Rudy Alvarado of UF ICBR Electron Microscopy core for their assistance with cryo-SEM and cryo-TEM. We would also like to thank Prof. Michael E. Harris and Kimberly C. Stevens for providing access to the CD machine and their assistance on the CD measurements. The content is solely the responsibility of the authors and does not necessarily represent the official views of the National Science Foundation or the National Institutes of Health.

© 2023 Wiley-VCH GmbH

15213773, 2023, 51, Downloaded from https://onlinelibrary.wiley.com/doi/10.1002/anie.202314531 by University Of Florida, Wiley Online Library on [06/08/2024]. See the Terms and Conditions (https://onlinelibrary.wiley.com/terms-and-conditions) on Wiley Online Library for rules of use; OA articles are governed by the applicable Creative Commons License

Conflict of Interest

The authors declare no conflict of interest.

Data Availability Statement

The data that support the findings of this study are available from the corresponding author upon reasonable request.

Keywords: Nanofibers · Peptide · Self-Assembly · Supramolecular Biomaterials

[1] S. Zhang, T. Holmes, C. Lockshin, A. Rich, *Proc. Natl. Acad. Sci. USA* **1993**, *90*, 3334–3338.

[2] a) G. M. Whitesides, B. Grzybowski, *Science* **2002**, *295*, 2418–2421; b) E. Gazit, *Chem. Soc. Rev.* **2007**, *36*, 1263–1269; c) R. Liu, G. A. Hudalla, *Molecules* **2019**, *24*, 1450.

[3] a) C. J. Bowerman, B. L. Nilsson, *Pept. Sci.* **2012**, *98*, 169–184; b) Y. Mandel-Gutfreund, L. M. Gregoret, *J. Mol. Biol.* **2002**, *323*, 453–461.

[4] a) J. Li, R. Xing, S. Bai, X. Yan, *Soft Matter* **2019**, *15*, 1704–1715; b) A. Dasgupta, J. H. Mondal, D. Das, *RSC Adv.* **2013**, *3*, 9117–9149.

[5] a) L. L. Li, Z. Y. Qiao, L. Wang, H. Wang, *Adv. Mater.* **2019**, *31*, 1804971; b) G. B. Qi, Y. J. Gao, L. Wang, H. Wang, *Adv. Mater.* **2018**, *30*, 1703444.

[6] a) Y. Li, F. Wang, H. Cui, *Bioeng. Transl. Med.* **2016**, *1*, 306–322; b) A. Yıldız, A. A. Kara, F. Acartürk, *Int. J. Biol. Macromol.* **2020**, *148*, 1084–1097; c) G. A. Hudalla, T. S. Sun, J. Z. Gasiorowski, H. Han, Y. F. Tian, A. S. Chong, J. H. Collier, *Nat. Mater.* **2014**, *13*, 829–836.

[7] a) J. Olguin, A. Restuccia, D. T. Seroski, G. A. Hudalla, *Peptide-based Biomaterials* **2020**, pp. 335–362; b) M. Barbosa, H. Simões, S. N. Pinto, A. S. Macedo, P. Fonte, D. M. F. Prazeres, *Acta Biomater.* **2022**, *143*, 216–232; c) A. Restuccia, Y. F. Tian, J. H. Collier, G. A. Hudalla, *Cell. Mol. Bioeng.* **2015**, *8*, 471–487; d) A. Restuccia, M. M. Fettis, S. A. Farhadi, M. D. Molinaro, B. Kane, G. A. Hudalla, *ACS Biomater. Sci. Eng.* **2018**, *4*, 3451–3459.

[8] a) C. Valéry, F. Artzner, M. Paternostre, *Soft Matter* **2011**, *7*, 9583–9594; b) X. Ma, Y. Zhao, C. He, X. Zhou, H. Qi, Y. Wang, C. Chen, D. Wang, J. Li, Y. Ke, *Nano Lett.* **2021**, *21*, 10199–10207.

[9] a) M. S. Lamm, K. Rajagopal, J. P. Schneider, D. J. Pochan, *J. Am. Chem. Soc.* **2005**, *127*, 16692–16700; b) H. Zhang, S. Lou, Z. Yu, *Langmuir* **2019**, *35*, 4710–4717.

[10] a) S. Vauthey, S. Santoso, H. Gong, N. Watson, S. Zhang, *Proc. Natl. Acad. Sci. USA* **2002**, *99*, 5355–5360; b) V. Haridas, *Acc. Chem. Res.* **2021**, *54*, 1934–1949.

[11] a) R. Huang, Y. Wang, W. Qi, R. Su, Z. He, *Nanoscale Res. Lett.* **2014**, *9*, 653; b) T. D. Jorgenson, M. Milligan, M. Sarikaya, R. M. Overney, *Soft Matter* **2019**, *15*, 7360–7368; c) S. Zhang, M. A. Greenfield, A. Mata, L. C. Palmer, R. Bitton, J. R. Mantei, C. Aparicio, M. Olvera de la Cruz, S. I. Stupp, *Nat. Mater.* **2010**, *9*, 594–601.

[12] a) A. Aggeli, M. Bell, L. M. Carrick, C. W. Fishwick, R. Harding, P. J. Mawer, S. E. Radford, A. E. Strong, N. Boden, *J. Am. Chem. Soc.* **2003**, *125*, 9619–9628; b) Y. Chen, H. X. Gan, Y. W. Tong, *Macromolecules* **2015**, *48*, 2647–2653.

[13] a) T. Shimada, K. Megley, M. Tirrell, A. Hotta, *Soft Matter* **2011**, *7*, 8856–8861; b) A. Kamada, A. Levin, Z. Toprakcioglu, Y. Shen, V. Lutz-Bueno, K. N. Baumann, P. Mohammadi, M. B. Linder, R. Mezzenga, T. P. Knowles, *Small* **2020**, *16*, 1904190.

[14] Y. Li, K. Li, X. Wang, B. An, M. Cui, J. Pu, S. Wei, S. Xue, H. Ye, Y. Zhao, *Nano Lett.* **2019**, *19*, 8399–8408.

[15] M. Wang, L. Du, X. Wu, S. Xiong, P. K. Chu, *ACS Nano* **2011**, *5*, 4448–4454.

[16] a) G. Pandey, J. Saikia, S. Sasidharan, D. C. Joshi, S. Thota, H. B. Nemade, N. Chaudhary, V. Ramakrishnan, *Sci. Rep.* **2017**, *7*, 2726; b) E. Radvar, Y. Shi, S. Grasso, C. J. Edwards-Gayle, X. Liu, M. S. Mauter, V. Castelletto, I. W. Hamley, M. J. Reece, H. S. Azevedo, *ACS Appl. Mater. Interfaces* **2020**, *12*, 22661–22672.

[17] a) R. Nelson, M. R. Sawaya, M. Balbirnie, A. O. Madsen, C. Riekel, R. Grothe, D. Eisenberg, *Nature* **2005**, *435*, 773–778; b) M. R. Sawaya, S. Sambashivan, R. Nelson, M. I. Ivanova, S. A. Sievers, M. I. Apostol, M. J. Thompson, M. Balbirnie, J. J. Wiltzius, H. T. McFarlane, A. O. Madsen, C. Riekel, D. Eisenberg, *Nature* **2007**, *447*, 453–457.

[18] a) D. R. Boyer, B. Li, C. Sun, W. Fan, K. Zhou, M. P. Hughes, M. R. Sawaya, L. Jiang, D. S. Eisenberg, *Proc. Natl. Acad. Sci. USA* **2020**, *117*, 3592–3602; b) R. Guerrero-Ferreira, N. M. Taylor, A.-A. Arteni, P. Kumari, D. Mona, P. Ringler, M. Britschgi, M. E. Lauer, A. Makky, J. Verasdonck, *eLife* **2019**, *8*, e48907.

[19] Y. Hu, R. Lin, P. Zhang, J. Fern, A. G. Cheetham, K. Patel, R. Schulman, C. Kan, H. Cui, *ACS Nano* **2016**, *10*, 880–888.

[20] A. Aggeli, M. Bell, N. Boden, L. M. Carrick, A. E. Strong, *Angew. Chem. Int. Ed.* **2003**, *42*, 5603–5606.

[21] a) J. R. Wester, J. A. Lewis, R. Freeman, H. Sai, L. C. Palmer, S. E. Henrich, S. I. Stupp, *J. Am. Chem. Soc.* **2020**, *142*, 12216–12225; b) R. Freeman, M. Han, Z. Álvarez, J. A. Lewis, J. R. Wester, N. Stephanopoulos, M. T. McClendon, C. Lynsky, J. M. Godbe, H. Sangji, *Science* **2018**, *362*, 808–813; c) X. Yang, H. Lu, B. Wu, H. Wang, *ACS Nano* **2022**, *16*, 18244–18252.

[22] a) X. Xie, T. Zheng, W. Li, *Macromol. Rapid Commun.* **2020**, *41*, 2000534; b) K. M. Wong, A. S. Robang, A. H. Lint, Y. Wang, X. Dong, X. Xiao, D. T. Seroski, R. Liu, Q. Shao, G. A. Hudalla, *J. Phys. Chem. B* **2021**, *125*, 13599–13609.

[23] P. Makam, E. Gazit, *Chem. Soc. Rev.* **2018**, *47*, 3406–3420.

[24] a) Q. Shao, K. M. Wong, D. T. Seroski, Y. Wang, R. Liu, A. K. Paravastu, G. A. Hudalla, C. K. Hall, *Proc. Natl. Acad. Sci. USA* **2020**, *117*, 4710–4717; b) K. M. Wong, Q. Shao, Y. Wang, D. T. Seroski, R. Liu, A. H. Lint, G. A. Hudalla, C. K. Hall, A. K. Paravastu, *J. Phys. Chem. B* **2021**, *125*, 4004–4015; c) K. M. Wong, Y. Wang, D. T. Seroski, G. E. Larkin, A. K. Mehta, G. A. Hudalla, C. K. Hall, A. K. Paravastu, *Nanoscale* **2020**, *12*, 4506–4518.

[25] D. T. Seroski, X. Dong, K. M. Wong, R. Liu, Q. Shao, A. K. Paravastu, C. K. Hall, G. A. Hudalla, *Commun. Chem.* **2020**, *3*, 172.

[26] a) B. Soto Morales, R. Liu, J. Olguin, A. M. Ziegler, S. M. Herrera, K. L. Backer-Kelley, K. L. Kelley, G. A. Hudalla, *Biomater. Sci.* **2021**, *9*, 2494–2507; b) L. Adler-Abramovich, P. Marco, Z. A. Arnon, R. C. Creasey, T. C. Michaels, A. Levin, D. J. Scurr, C. J. Roberts, T. P. Knowles, S. J. Tendler, *ACS Nano* **2016**, *10*, 7436–7442.

[27] M. Cheon, I. Chang, C. K. Hall, *Proteins Struct. Funct. Bioinf.* **2010**, *78*, 2950–2960.

[28] D. T. Seroski, A. Restuccia, A. D. Sorrentino, K. R. Knox, S. J. Hagen, G. A. Hudalla, *Cell. Mol. Bioeng.* **2016**, *9*, 335–350.

[29] L. A. Feigin, D. I. Svergun, *Structure analysis by small-angle X-ray and neutron scattering, Vol. 1*, Plenum Press, New York, **1987**.

[30] A. Restuccia, D. T. Seroski, K. L. Kelley, C. S. O'Bryan, J. J. Kurian, K. R. Knox, S. A. Farhadi, T. E. Angelini, G. A. Hudalla, *Commun. Chem.* **2019**, *2*, 53.

© 2023 Wiley-VCH GmbH

15213773, 2023, 51, Downloaded from https://onlinelibrary.wiley.com/doi/10.1002/anie.202314531 by University Of Florida, Wiley Online Library on [06/08/2024]. See the Terms and Conditions (https://onlinelibrary.wiley.com/terms-and-conditions) on Wiley Online Library for rules of use; OA articles are governed by the applicable Creative Commons License

[31] C. Yuan, A. Levin, W. Chen, R. Xing, Q. Zou, T. W. Herling, P. K. Challa, T. P. Knowles, X. Yan, *Angew. Chem.* **2019**, *131*, 18284–18291.
[32] A. Huerta-Viga, S. Amirjalayer, S. R. Domingos, H. Meuzelaar, A. Rupenyan, S. Woutersen, *J. Chem. Phys.* **2015**, *142*, 212444.
[33] G. Zandomeneghi, M. R. Krebs, M. G. McCammon, M. Fandrich, *Protein Sci.* **2004**, *13*, 3314–3321.
[34] G. Meisl, J. B. Kirkegaard, P. Arosio, T. C. Michaels, M. Vendruscolo, C. M. Dobson, S. Linse, T. P. Knowles, *Nat. Protoc.* **2016**, *11*, 252–272.
[35] a) J. Wang, K. Liu, R. Xing, X. Yan, *Chem. Soc. Rev.* **2016**, *45*, 5589–5604; b) R. Zuo, R. Liu, J. Olguin, G. A. Hudalla, *J. Phys. Chem. B* **2021**, *125*, 6559–6571.
[36] a) K. E. Drzewiecki, D. R. Grisham, A. S. Parmar, V. Nanda, D. I. Shreiber, *Biophys. J.* **2016**, *111*, 2377–2386; b) K. E. Drzewiecki, A. S. Parmar, I. D. Gaudet, J. R. Branch, D. H. Pike, V. Nanda, D. I. Shreiber, *Langmuir* **2014**, *30*, 11204–11211.
[37] N. Makarava, O. V. Bocharova, V. V. Salnikov, L. Breydo, M. Anderson, I. V. Baskakov, *Protein Sci.* **2006**, *15*, 1334–1341.
[38] R. Jansen, W. Dzwolak, R. Winter, *Biophys. J.* **2005**, *88*, 1344–1353.
[39] S. S. Rogers, M. R. Krebs, E. H. Bromley, E. van der Linden, A. M. Donald, *Biophys. J.* **2006**, *90*, 1043–1054.
[40] X. Yu, A. Carlsson, *Biophys. J.* **2004**, *87*, 3679–3689.
[41] X. Du, J. Zhou, J. Shi, B. Xu, *Chem. Rev.* **2015**, *115*, 13165–13307.
[42] R. Gallardo, N. A. Ranson, S. E. Radford, *Curr. Opin. Struct. Biol.* **2020**, *60*, 7–16.
[43] Y. Yang, R. B. Meyer, M. F. Hagan, *Phys. Rev. Lett.* **2010**, *104*, 258102.
[44] T. M. Clover, C. L. O'Neill, R. Appavu, G. Lokhande, A. K. Gaharwar, A. E. Posey, M. A. White, J. S. Rudra, *J. Am. Chem. Soc.* **2020**, *142*, 19809–19813.
[45] C. B. Andersen, H. Yagi, M. Manno, V. Martorana, T. Ban, G. Christiansen, D. E. Otzen, Y. Goto, C. Rischel, *Biophys. J.* **2009**, *96*, 1529–1536.
[46] X. Dong, R. Liu, D. T. Seroski, G. A. Hudalla, C. K. Hall, *PLOS Comp. Biol.*, *in press* .
[47] Y. Fezoui, D. B. Teplow, *J. Biol. Chem.* **2002**, *277*, 36948–36954.
[48] J. L. Regier, F. Shen, S. J. Triezenberg, *Proc. Natl. Acad. Sci. USA* **1993**, *90*, 883–887.
[49] A. Chakrabartty, A. J. Doig, R. L. Baldwin, *Proc. Natl. Acad. Sci. USA* **1993**, *90*, 11332–11336.
[50] T. Lemke, M. Edte, D. Gebauer, C. Peter, *J. Phys. Chem. B* **2021**, *125*, 10335–10343.
[51] a) D. M. Hall, I. R. Bruss, J. R. Barone, G. M. Grason, *Nat. Mater.* **2016**, *15*, 727–732; b) A. Aggeli, I. A. Nyrkova, M. Bell, R. Harding, L. Carrick, T. C. McLeish, A. N. Semenov, N. Boden, *Proc. Natl. Acad. Sci. USA* **2001**, *98*, 11857–11862.
[52] D. R. Boyer, N. A. Mynhier, M. R. Sawaya, *BioRxiv preprint* **2021**, 2021.2007. 2002.450971.
[53] J. Adamcik, R. Mezzenga, *Soft Matter* **2011**, *7*, 5437–5443.

Manuscript received: September 27, 2023
Accepted manuscript online: November 6, 2023
Version of record online: November 20, 2023

© 2023 Wiley-VCH GmbH

15213773, 2023, 51, Downloaded from https://onlinelibrary.wiley.com/doi/10.1002/anie.202314531 by University Of Florida, Wiley Online Library on [06/08/2024]. See the Terms and Conditions (https://onlinelibrary.wiley.com/terms-and-conditions) on Wiley Online Library for rules of use; OA articles are governed by the applicable Creative Commons License